IOP Publishing Journal Title
Journal **XX** (XXXX) XXXXXX https://doi.org/XXXX/XXXX

1
2
3
4
5
6
7
8
9
10

Computer simulation of the operational characteristics of a microstrip silicon detector

11
12
13
14
15
16
17
18
19
20
21

Ivan Lovshenko[1], Polina Roshchenko[1], Veranika Shandarovich[1], Viktor Stempitsky[1], Tran Tuan Trung[2] and Dao Dinh Ha[2]

[1] Micro- and Nanoelectronics, Belarusian State University of Informatics and Radioelectronics, Minsk, Belarus
[2] Microprocessor Engineering, Le Quy Don Technical University, Hanoi, Vietnam

E-mail: daodinhha@mta.edu.vn

22
23
24
25

Received xxxxxx
Accepted for publication xxxxxx
Published xxxxxx

26
27
28
29
30
31
32
33
34
35
36
37

Abstract

The paper presents the results of an analysis of the operational characteristics of semiconductor microstrip detectors (SMD) using methods and software for device-technological simulation. The effect on the characteristics of a detector of heavy charged particles (HCP) with a linear energy transfer (LET) of 1.81 MeV·cm^2/mg, 18.8 MeV·cm^2/mg and 55.0 MeV·cm^2/mg, corresponding to nitrogen ions $^{15}N^{+4}$, was studied with an energy of E = 1.87 MeV, iron ions $^{56}Fe^{+15}$ with an energy of E = 523 MeV and xenon $^{131}Xe^{+35}$ with an energy of E = 1217 MeV, as well as the angle of incidence of the particle λ and the values of temperature and voltage on the substrate. To improve the characteristics of a detector, a screening experiment was carried out and a series of optimization calculations were performed.

38
39
40
41
42
43

Keywords: microstrip detector, device simulation, radiation, single event upset, linear energy transfer

44
45
46
47
48
49
50
51
52
53
54
55
56
57
58
59
60

1. INTRODUCTION

Research in the field of high energy physics (HEP) and cosmic ray physics (CRP) requires the use of a large number of methods for recording and identifying particles, measuring their energy, trajectory, and place of formation. To select methods, it is important to consider criteria such as practical feasibility, accuracy and limitations on their use. For a long time, one of the main methods was considered to be the registration of particles using gas-filled coordinate detectors. The principle of operation of such detectors is the phenomenon caused by the interaction of radiation with matter, which produces the ionization of atoms and molecules along the particle's track through the material. Thus, the generated charge carriers (ion pairs) are collected by electrodes and read by electronic equipment [1]. In studies in the CRP, where radiation loads are several orders of magnitude less, and the required read speed does not exceed several tens of events per second (against $10^5..10^7$ 1/s in the PVE), there are problems for which recording devices with "unique" parameters are needed. For example, spatial resolution with extremely high multiplicity of processes. Also an urgent task is to determine the chemical composition of cosmic rays.

However, with the development of physical experiments using colliders (LHC – large hadron collider, ILC - international linear collider, SLHC – super large hadron collider, RHIC – heavy ion collider, etc.), as well as experiments with ion beams, their operational characteristics are insufficient to meet all the needs of modern tasks [2]. Recently, gas-filled coordinate detectors have been replaced by semiconductor detectors, which provide registration of particles, restoration of their tracks and secondary decay vertices at a high response rate. In addition, such detectors

 © xxxx IOP Publishing Ltd

1 2 3 4 5 6 7 8 9 10 11 12 13 14 15 16 17 18 19 20 21 22 23 24 25 26 27 28 29 30 31 32 33 34 35 36 37 38 39 40 41 42 43 44 45 46 47 48 49 50 51 52 53 54 55 56 57 58 59 60

provide the best accuracy in determining the coordinates of particles in detecting systems that can operate in strong magnetic fields and in harsh radiation conditions [3, 4].

Regardless of the mechanism of electron-hole pair formation, a single charged particle spends the same average energy to create one pair, the value of which for SD from silicon and germanium is 3.7 eV and 2.9 eV, respectively (for gas detectors, the energy necessary to create ion pairs, equal to 30 eV) [5]. Also, the advantages of semiconductor detectors include ensuring accurate position measurement with a high reading speed, direct accessibility of signals in electrical form, accurate measurements of energy and trajectories at the same time, and, finally, the possibility of integrating the detector and readout electronics onto a common substrate.

General requirements for semiconductor detectors are: linearity between the radiation power and the number of electron-hole pairs; low leakage current; generation of the maximum number of electron-hole pairs per radiation unit; high detection efficiency; low cost [6]. When designing and during operation of the semiconductor detectors, it is necessary to take into account the presence of a dead zone and the possibility of radiation damage to the device.

To fix the trajectory of the charged particle, semiconductor microstrip detectors (SMD) are used, which are made on single-crystal silicon wafers using standard microelectronic technologies. The key parameters of SMD are spatial and temporal resolution, dead time and registration efficiency. In addition to semiconductor detectors, the requirements are met by artificial diamond detectors, however, the unworked technology of growing the material and the actual manufacture of the detectors and the high cost of production do not allow the use of these devices in real installations [7, 8].

The development of the design, circuitry, and topological solutions of SMD for use in the HEP and CRP requires large material and time resources. Modern computer-aided design software systems in microelectronics (for example, Silvaco [9] and Synopsys [10]) make it possible to evaluate the characteristics of detectors based on the geometry, materials used and the technological process of formation, without actually making them. Despite the widespread use of silicon microstrip detectors in studies of PVE, further application in future high-luminosity colliders requires solving problems related to the degradation of their characteristics when operating under severe radiation conditions, which reduces the efficiency of charge carrier collection [11]. To compensate for such changes, the bias voltage of the detector is gradually increased, which leads to an increase in leakage currents, an increase in temperature and power, and a decrease in the signal-to-noise ratio [12]. In this case, the leakage current in the instrument structure is unevenly distributed. Therefore, it is important to detect areas in which leakage can develop and to compare them with the geometric and technological parameters of the instrument structure. This problem can be solved by computer simulation, the application of which allows you to take into account such radiation effects as TID, DD or SEE, providing an analysis of the characteristics of the detector after radiation exposure.

This work is dedicated to solving an important problem associated with the development of silicon detectors for high-energy physics and cosmic ray physics using computer-aided design systems in microelectronics. The aim of the work is the application of computer simulation methods to assess the operational characteristics of semiconductor microstrip detectors taking into account the effects of heavy charged particles.

2. STRUCTURE MICROSTRIPS DETECTORS

The standard SMD signal readout circuit (Fig. 1.) implies the presence of a bias resistor and an isolation capacitor (to isolate the amplifier input from a high bias voltage) for each read channel. The signal from the capacitor is fed to a charge-sensitive amplifier with a signal to noise ratio of at least 20. The number of such amplifiers is equal to the number of channels of the microstrip detector. Due to technological limitations, the placement of capacitors and high-resistance resistors in the IC of an amplifier is impossible, these elements are integrated into a microstrip detector. On the periphery of the microstrip detector with capacitive signal pick-up, p^+-guard rings are placed, a common power bus (voltage 0 V), to which mixing resistors are connected (resistance value is taken from 0.5 to 3 MΩ) made of polycrystalline silicon. Capacitors form over the strip. A double insulating layer of SiO_2/Si_3N_4 acts as a dielectric. The spatial resolution of SMD is determined by the step of the read strips (L). The accuracy of reading spatial coordinates can be improved by using special algorithms for measuring the signal amplitude in each channel and by placing strips between the readable strips that are not connected to the readout electronics (non-readable) [13].

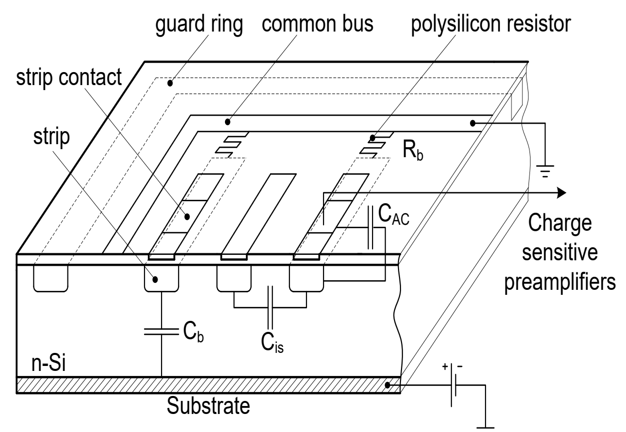

Fig. 1. Diagram of a microstrip detector with capacitive signal pickup

The structure of a microstyp detector, which includes three strip contacts (SC) located on the surface of a silicon wafer of an electronic type of electrical conductivity with a thickness of 300 μm (impurity concentration equal to 10^{16} cm^{-3}), was chosen as the object of study [14, 15]. The contact regions of the SC silicon wafer are doped with an acceptor impurity to a concentration of 10^{18} cm^{-3}. On the reverse side is the contact of the substrate (the contact regions of the silicon wafer are additionally doped with a donor impurity to a concentration of 10^{18} cm^{-3}).

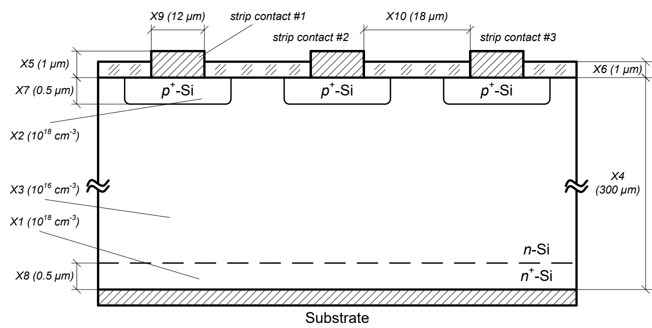

Fig. 2. SMD unit cell structure

For the simulation of the technological process for the formation of the SMD structure with design rules of 1.5 μm, 7 stages are conventionally assigned: setting the substrate and the computational grid, forming an n^+-hidden layer (ion implantation of As), metallization (forming an aluminum contact to current electrodes), oxidizing the substrate for implantation boron, oxide etching to create windows for contacts, doping of p^+-regions (ion implantation of boron, distillation of impurities), deposition of an aluminum film and the formation of aluminum contacts (etching). The structure of the device with designated contacts and areas is shown in Fig. 2 (the values of the parameters of basic device structure are indicated in brackets). The simulation setup did not take into account the influence of strips adjacent to the unit cell and the edge effects at the ends of the strips.

Preliminary simulation results showed that the use of default models does not fully meet the requirements for modeling accuracy. Based on the calculation results, the Shockley-Reed-Hall recombination model (srh), the mobility model based on the look-up table (conmob) and the parallel-dependent electric field component (fldmob), the standard Auger recombination model, and the charge carrier statistics model were additionally selected taking into account the narrowing of the band gap (bgn), the model of impact ionization Selberher (Selberherr).

For the obtained structure, it was found that for the nominal modes of technological operations and design parameters, the breakdown voltage is 45 V. The leakage currents for each of the SCs at a voltage on the substrate of 10 V do not exceed $5 \cdot 10^{-14}$ A.

3. RESULTS

Through of computer-aided design systems in microelectronics, the effect of a heavy charged particle (HCP) on the electrical characteristics of the instrumental structure of SMD with variation in the angle of incidence λ (entry point is located between SCs 2 and 3) was investigated. Simulation conditions: voltage on SCs 1-3 is 0 V, voltage on the substrate is 10 V; the ambient temperature is 273 K. Particles with LET equal to 1.81 MeV·cm^2/mg, 18.8 MeV·cm^2/mg and 55.0 MeV·cm^2/mg corresponding to $^{15}N^{+4}$ nitrogen ions with energy E = 1.87 MeV, iron $^{56}Fe^{+15}$ with an energy of E = 523 MeV and xenon $^{131}Xe^{+35}$ with an energy of E = 1217 MeV. The impact on the instrument structure peaks at 10 ps and has a Gaussian time profile with a characteristic value of 1 ps. Carrier generation occurs along the entire particle track length (from y = -1 μm to y = 301 μm) within the nominal radius of the 0.05 μm axis of the track at a density of 10^{18} electron-hole pairs per cm^3.

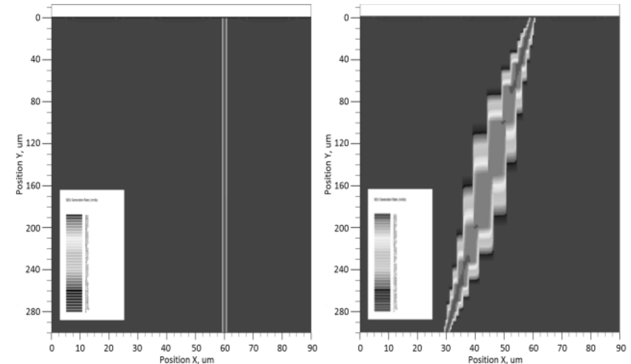

Fig. 3. The rate of generation of charge carriers along a particle track with an incidence angle of λ = 0º (a) and λ = 5.7º (b) at a temperature of 273 K.

The carrier generation rate along the particle track at a temperature of 273 K and for angles λ = 0º and λ = 5.7º is shown in Fig. 3. The maximum value in the center of the track is $2 \cdot 10^{29}$ $cm^{-3} \cdot s^{-1}$.

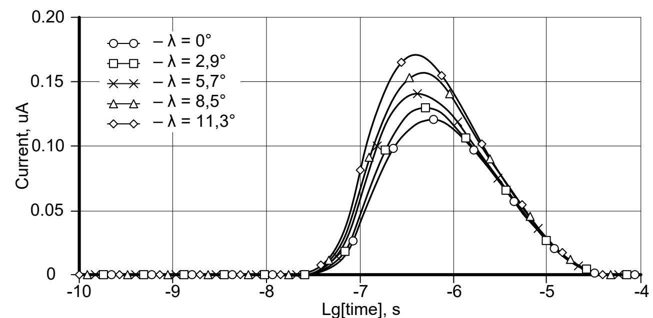

Fig. 4. Time dependence of the current through the SC 1 when exposed HCP 15N^{+4} nitrogen at a temperature of 273 K, and variation of the angle λ

The time dependencies for the current through SC 1 under the action of a TLC of nitrogen $^{15}N^{+4}$ at a temperature of 273 K and a variation in the angle λ are presented in Fig. 4. The current of SC 1 at a time equal to 0.6 μs reaches its maximum of 0.12 μA, 1.58 μA, and 5.39 μA for nitrogen $^{15}N^{+4}$, iron $^{56}Fe^{+15}$, and xenon $^{131}Xe^{+35}$, respectively. The ratio of the maximum current of SC 1 I1 to the maximum current of SC 2 (3) I_2 (I_3) is 0.053 (0.052), 0.05 (0.05), 0.049 (0.048), respectively, for nitrogen $^{15}N^{+4}$, iron $^{56}Fe^{+15}$ and xenon $^{131}Xe^{+35}$. Thus, the ratio I_1/I_2 decreases with increasing LET of the particle.

It was found that at an angle λ = 0º and a temperature of T = 273 K, the values of the current through SCs 2 and 3 practically coincide regardless of the current transformer. Table I presents the parameters of the instrumental structure of SMD with variation of the particle and its angle of incidence λ for SCs 2 and 3.

An analysis of the values given in Table I shows a nonlinear dependence of the magnitude of the I_{3MAX}/I_{2MAX} ratio on the angle of incidence of the particle, regardless of its LET. This feature requires the use of a special software algorithm or hardware solution of the reading system. For the case under consideration, it is proposed to use the dependence of the ratio I_{3MAX}/I_{2MAX} on the angle of incidence of the particle and its LET:

$$\lambda = (I_{3MAX}/I_{2MAX} - B)/A \qquad (1)$$

where A and B are coefficients reflecting the dependence of the maximum values of currents through strip contacts on LET, calculated on the basis of empirical expressions

$$A = -0.001 \cdot \ln(LET) + 0.0431 \qquad (2)$$

$$B = -0.003 \cdot \ln(LET) + 1.0285 \qquad (3)$$

The reliability of the approximation when using these expressions is at least 0.96.

TABLE I. RESULTS OF CHARACTERISTICS SIMULATION UNDER EXPOSURE TO HCP AND CHANGE OF FALL ANGLE λ

HCP	Parameter	Angle λ, deg				
		0	2,9	5,7	8,5	11,3
$^{15}N^{+4}$	I_{2MAX}, uA	2,25	2,49	2,38	3,13	3,21
	I_{3MAX}, uA	2,27	2,32	1,76	2,04	1,83
	I_{3MAX} / I_{2MAX}	1,009	0,932	0,740	0,652	0,570
	Deviation of I_{3MAX} / I_{2MAX} from the previous value, %	0	-7,63	-20,60	-11,89	-12,57
$^{56}Fe^{+15}$	I_{2MAX}, uA	31,60	33,98	33,32	42,85	43,90
	I_{3MAX}, uA	31,70	31,61	24,91	28,64	25,75
	I_{3MAX} / I_{2MAX}	1,003	0,930	0,748	0,668	0,587
	Deviation of I_{3MAX} / I_{2MAX} from the previous value, %	0	-7,28	-19,57	-10,69	-12,13
$^{131}Xe^{+35}$	I_{2MAX}, uA	101	109	107	136	139
	I_{3MAX}, uA	101	101	80	92	83
	I_{3MAX} / I_{2MAX}	1,002	0,927	0,748	0,677	0,597
	Deviation of I_{3MAX} / I_{2MAX} from the previous value, %	0	-7,49	-19,31	-9,49	-11,82

With an increase in the LET of a particle, an increase in the I_{3MAX}/I_{2MAX} ratio is observed (except for the case with λ = 2.9º), which is explained by the large number of generated charge carriers along the particle track and their redistribution in the device structure before collection by strip contacts and the substrate contact.

A study was made of the effect of temperature on the magnitude of the currents through SCs 2 and 3 when exposed to an electric current transformer at different angles of incidence. The calculation result for the case λ = 5.7º is shown in Fig. 5. It was shown that under the action of nitrogen $^{15}N^{+4}$ HCP on the SMD structure with decreasing temperature, the currents through SCs 2 and 3 increase unequally, both expressed in absolute and in relative values (Table II). It was also established that with decreasing temperature, the rate of change of the current magnitudes increases. So, for SC 2, the maximum current rises by 14.29 %, 15 %, 19.57 %, 25.45 % with a decrease in temperature to 223 K, 173 K, 123 K, 73 K, respectively, relative to the previous value. The described features must be taken into account when conducting field experiments. For the remaining particles, a similar dependence of SCs 2–3 currents on temperature is observed. To obtain more accurate results at temperatures below 100 K, additional models of incomplete ionization of the impurity are necessary.

A study was made of the effect of voltage on the substrate on the magnitude of currents through SCs 2 and 3 when exposed to $^{15}N^{+4}$ HCP of nitrogen at angles λ = 0º and λ = 11.3º and T = 273 K. The calculation result for the case λ = 11.3º shown in Fig. 6.

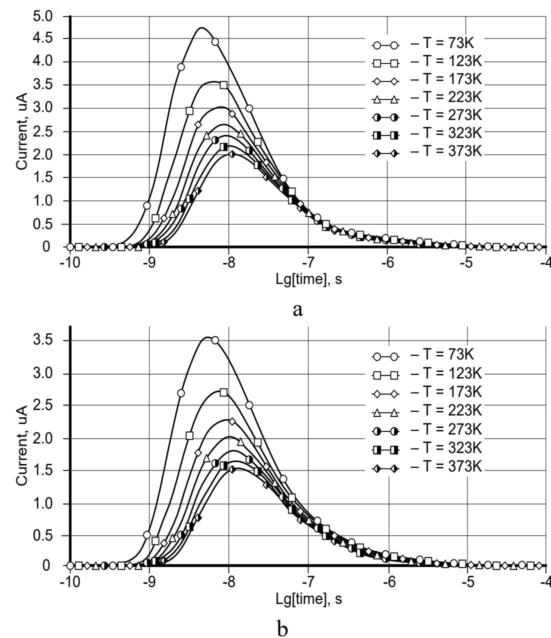

Fig. 5. Time dependencies of the current through SCs 2 (a) and 3 (b) when exposed to the HCP of nitrogen 15N+4 at λ = 5.7º and temperature variations.

TABLE II. RESULTS OF CHARACTERISTICS SIMULATION UNDER THE INFLUENCE OF HCP AND CHANGE OF TEMPERATURE

HCP	Parameter	Temperature, K						
		73	123	173	223	273	323	373
$^{15}N^{+4}$	I_{2MAX}, uA	4,27	3,51	3,02	2,66	2,38	2,15	1,96
	ΔI_{2MAX}, %	21,65	16,23	13,53	11,77	0	-9,66	-8,84
	I_{3MAX}, uA	3,4	2,73	2,3	1,99	1,76	1,57	1,42
	ΔI_{3MAX}, %	24,54	18,70	15,58	13,07	0	-10,80	-9,55
	I_{3MAX} / I_{2MAX}	0,796	0,778	0,762	0,748	0,740	0,730	0,725
$^{56}Fe^{+15}$	I_{2MAX}, uA	57,91	48,41	42	37,16	33,32	30,2	27,58
	ΔI_{2MAX}, %	19,62	15,26	13,03	11,53	0	-9,36	-8,68
	I_{3MAX}, uA	46,49	37,9	32,25	28,11	24,91	22,34	20,22
	ΔI_{3MAX}, %	22,67	17,52	14,73	12,85	0	-10,32	-9,49
	I_{3MAX} / I_{2MAX}	0,800	0,783	0,768	0,757	0,748	0,740	0,733
$^{131}Xe^{+35}$	I_{2MAX}, uA	188	157	136	119	107	97	88
	ΔI_{2MAX}, %	19,75	15,44	14,29	11,22	0	-9,35	-9,28
	I_{3MAX}, uA	151	124	105	91	80	72	65
	ΔI_{3MAX}, %	21,77	18,10	15,39	13,75	0	-10	-9,72
	I_{3MAX} / I_{2MAX}	0,803	0,790	0,772	0,765	0,748	0,742	0,739

It is shown that under the action of nitrogen $^{15}N^{+4}$ HCP on the SMD structure (angle value $\lambda = 11.3^{o}$), an increase in voltage by 10 V (from 10 V to 20 V) leads to an increase in currents of SC 2 by 15.63 % and SC 3 by 16.21 %. With a further increase in voltage to 30 V and 40 V, the currents increase by 21.62 % and 13.33 % for SC 2, by 13.95 % and 10.42 % for SC 3, respectively. The current SC 1 in this case is practically independent of the voltage on the substrate. So, at a voltage on the substrate of 10 V and 40 V, the maximum current of SC 1 is 0.169 μA and 0.171 μA, respectively. For the rest of the HCP, the same dependence is observed.

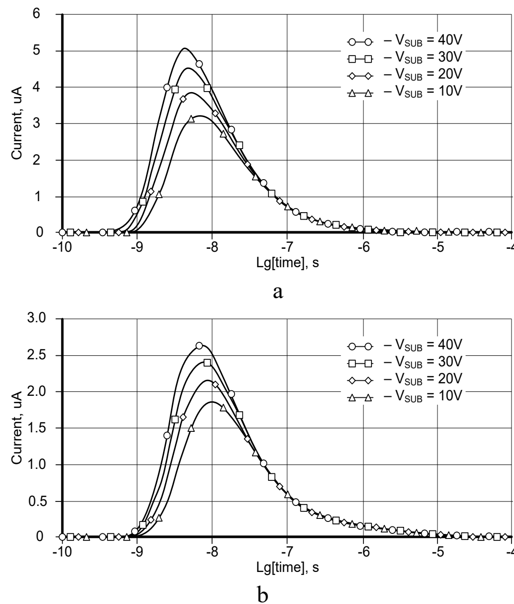

Fig. 6.Time dependencies of the current through SCs 2 (a) and 3 (b) under the action of a 15N+4 HCP at $\lambda = 11.3^{o}$, a temperature of 273 K, and voltage variations on the substrate.

The dependence of the temporal resolution Y of the PMD instrument structure on the angle λ (Fig. 7.), temperature (Fig. 8.) and substrate voltage (Fig. 9.) under the influence of HCP of iron $^{56}Fe^{+15}$ with an energy E = 523 MeV is estimated.

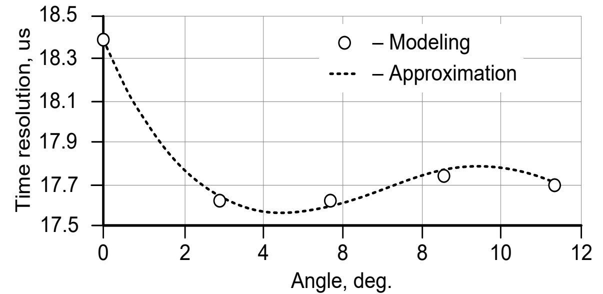

Fig. 7. The dependence of the time resolution on the angle of incidence of the particle.

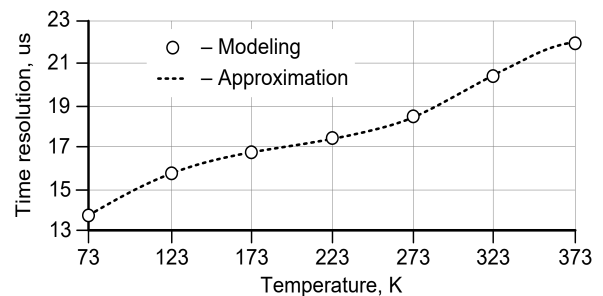

Fig. 8. The dependence of the temporal resolution of the temperature.

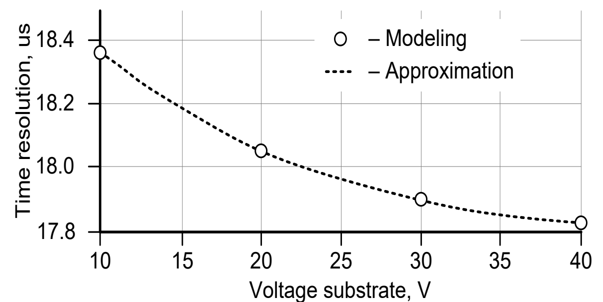

Fig. 9. The dependence of the temporal resolution of the substrate voltage.

An analysis of the obtained dependencies of the temporal resolution Y of SMD on the angle λ (when exposed to HCP of iron $^{56}Fe^{+15}$ and T = 273 K) and the voltage on the substrate ($\lambda = 0^{o}$, T = 273 K) allows us to conclude that these parameters have weak effect on the value of time resolution. Thus, the limiting values of the time resolution with a variation of the angle λ from 0° to 11.3^{o} are $1.76 \cdot 10^{-5}$ s and $1.84 \cdot 10^{-5}$ s, with a variation in the voltage on the substrate - $1.79 \cdot 10^{-5}$ s and $1.84 \cdot 10^{-5}$ s. To reduce the temporal resolution, it is necessary to strive to lower the temperature during research. So, at a temperature of T = 273 K and T = 73 K, the temporal resolution is $2.19 \cdot 10^{-5}$ s and $1.38 \cdot 10^{-5}$ s, respectively.

4. OPTIMIZATION

To determine the design parameters and modes of technological operations for the formation of SMD, which have the greatest impact on characteristics, a screening experiment was carried out according to the Plackett-Berman plan using the Hadamard matrix [16, 17]. The criterion for a screening experiment is a temporal resolution (Y). The input factors influencing on this parameter are: donors concentration (factor X1); acceptors concentration (factor X2); impurity concentration in the substrate (factor X3); substrate thickness (factor X4); SC thickness (factor X5); oxide thickness (factor X6); depth of occurrence of a p-n-junction (factor X7); depth of occurrence of implanted arsenic impurity (factor X8); SK width (factor X9); distance between SC (factor X10). Figure 2 provides an explanation of the selected factors.

Because of the screening experiment, it was found that a design and technological parameters that have a greatest impact on the temporal resolution are: substrate thickness (factor X4); SK width (factor X9); distance between SC (factor X10).

Fig. 10–12 show the dependences of the temporal resolution when the value of the most significant factors changes, as well as the approximating equations with the corresponding values of the approximation reliability R^2.

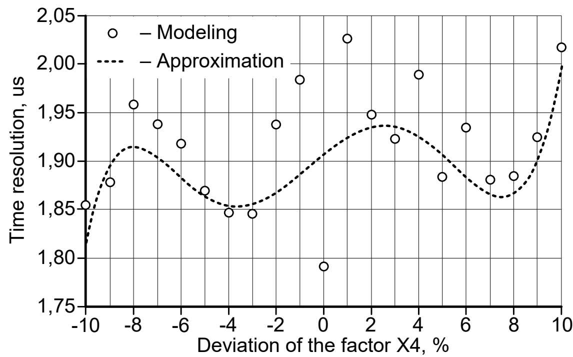

Fig. 10. Dependence of the temporal resolution on the deviation of the factor X4

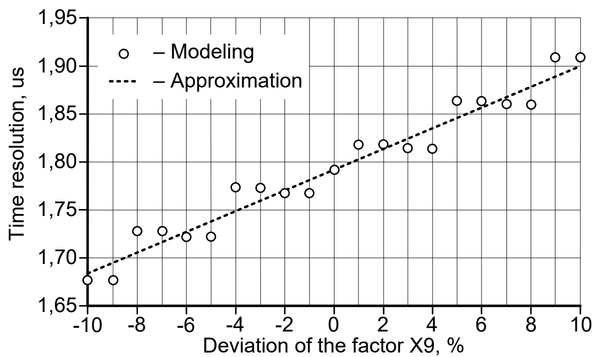

Fig. 11. Dependence of the temporal resolution on the deviation of the factor X9

Based on the data obtained, it can be concluded that the temporal resolution is linearly dependent on the SC width (factor X9) and the distance between the SC (factor X10). The effect of the substrate thickness parameter (factor X4) on the temporal resolution is more complex.

The procedure for optimizing the design and technological parameters of the device structure of the SMD was reduced to the mathematical problem of determining the values of significant input factors (X4, X9, X10) in the range of values from 0.9 to 1.1 in relation to the nominal value, providing a decrease in the temporal resolution by 10% in relation to the nominal. Optimization was carried out using a modified Levenberg-Marquart algorithm used to construct a response surface describing the dependence between input parameters and output characteristic in an iterative process.

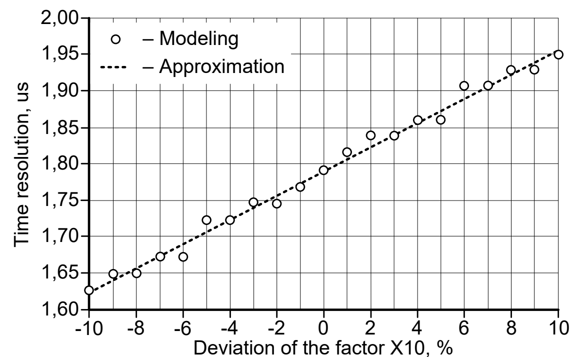

Fig. 12. Dependence of the temporal resolution on the deviation of the factor X10

Fig. 13 shows the dependences of the current through SC №1–3 on time for the structure with nominal (dotted line) and optimized (solid line) parameter values.

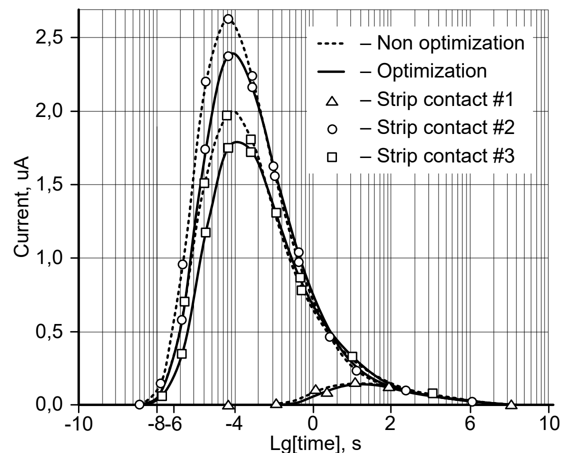

Fig. 13. Dependences of the current through SC on time for the structure with nominal and optimized parameter values

Because of optimization calculations, the values of design and technological parameters (X4 = 300 μm, X9 = 10.8 μm, X10 = 16.2 μm) were obtained, which ensured a decrease in

1
2
3
4
5
6
7
8
9
10
11
12
13
14
15
16
17
18
19
20
21
22
23
24
25
26
27
28
29
30
31
32
33
34
35
36
37
38
39
40
41
42
43
44
45
46
47
48
49
50
51
52
53
54
55
56
57
58
59
60

the temporal resolution by 277 ns, which is 15.5% of the nominal value. In this case, the maximum decrease in the value of currents through SC №1–3 is observed for SC №2 and amounts to 0.95% (from 2.63 μA to 2.38 μA).

5. CONCLUSION

The technological route for the formation of the SMD instrument structure with design standards of 1.5 μm was simulated, for which the breakdown voltage is 45 V and the leakage current of strip contacts at a voltage of 10 V on the substrate does not exceed $5 \cdot 10^{-14}$ A. The current value of the strip contacts, between which the input point of the HCP, is more than 8 orders of magnitude higher than the leakage current without the influence of the HCP. It was established that at an angle of incidence of $\lambda = 0°$, the magnitudes of these currents practically coincide irrespective of the HCP.

A nonlinear dependence of the magnitude of the ratio of currents on the angle of incidence of the particle is established, regardless of its LET, which necessitates the use of special techniques in the reading system. For the case under consideration, an expression is proposed for determining the angle of incidence of a particle from the ratio of currents with an approximation reliability of at least 0.96.

It is shown that a decrease in temperature leads to an inhomogeneous increase in the currents through the SC, an increase in the rate of change of the current values. So, for SC 2, the maximum current rises by 14.29 %, 15 %, 19.57 %, 25.45 % with a decrease in temperature to 223 K, 173 K, 123 K, 73 K, respectively, relative to the previous value. The described features must be taken into account when conducting field experiments. To obtain more accurate results at temperatures below 100 K, additional models of incomplete ionization of the impurity are necessary.

In the study of the effect of voltage on the substrate on the magnitude of the currents through the SC, it is shown that with an increase in voltage by 10 V leads to an increase in currents by more than 15 %. The SC current, in the region of which the particle trajectory does not lie, is practically independent of the voltage on the substrate. So, with a voltage on the substrate of 10 V and 40 V, the maximum current is 0.169 μA and 0.171 μA, respectively.

It is shown that in order to obtain the best time resolution, it is necessary to reduce the temperature in the chamber in which the measurement takes place and increase the voltage on the substrate.

The results of the screening experiment to determine the design and technological parameters that have the greatest impact on the temporal resolution of the SMD are presented. These parameters are the thickness substrate (factor X4), SK width (factor X9) and distance between SK (factor X10). Because of optimization calculations using the modified Levenberg-Marquart algorithm, the values of these parameters were obtained, which ensure a decrease in the value of the temporal resolution by 15.5% of the nominal value.

Acknowledgements

The work was supported by a grant from the Belarusian State Research Program "Photonics, opto- and microelectronics" (Tasks 3.1.03).

References

[1] J. Fraden, Handbook of Modern Sensors: Physics, Designs, and Applications. Fraden Corp.San Diego, CA, USA: Springer, 2016, 758 p.

[2] P. Allport "Applications of silicon strip and pixel-based particle tracking detectors" in Nature Reviews Physics, vol. 1, 2019, pp. 567-576.

[3] M. Bagatin, S. Gerardin, Ionizing radiation effects in electronics: From Memories to Imagers. Boca Raton: CRC Press, 2016, 378 p.

[4] M. Merkin, "Razrabotka, sozdanie i primenenie kremnievyh detektorov v fizike vysokih energij i fizike kosmicheskih luchej : avtoreferat," Moscow: MGU, 2012, 285 p. [in Russian]

[5] G. F. Knoll, Radiation detection and measurement. Hoboken, New Jersey: Wiley , 2010, 864 p.

[6] Yu. A. Rodionov, "Mikroelektronnye datchiki i sensornye ustrojstva: ucheb. posobie," Minsk: BSUIR, 2019, 300 p. [in Russian]

[7] V. B. Kvaskov, "Almaz v elektronnoj tekhnike," Moscow: Energoatomizdat, 1990, 248 p. [in Russian]

[8] S. Kumar, "Comparative Study of Radiation damage in Si, Ge and Diamond used as Detector" in Proceedings of the DAE-BRNS Symp. on Nucl. Phys. 61, 2016, pp. 1076-1077.

[9] Silvaco [Electronic resource]. - Access mode: http://silvaco.com/. - Access date: 06.07.2020.

[10] Synopsys [Electronic resource]. - Access mode: http://synopsys.com/. - Access date: 06.07.2020.

[11] D. Passeri, P. Ciampolini, G. M. Bilei, "A comprehensive analysis of low-resistivity radiation detectors," IEEE Trans. on Nuclear Science, vol. 46, n.3, pp. 260-265, June 1999.

[12] CMS Collaboration, "CMS Technical Design Report," CERN, Ginevra, Switzerland, May 1998.

[13] S. G. Basiladze, G. A. Bogdanova, M. V. Vasil'ev, "Elektronnaya apparatura s'ema i registracii signalov s mikrostripovogo vershinnogo detektora ustanovki SVD-2," in PTE, 2006, vol. 3, pp. 52-60.

[14] G. Lutz, "Semiconductor Radiation Detectors," Berlin: Springer, 2007, 353 p.

[15] A. Owens. "Compound Semiconductor Radiation Detectors," Boca Raton: CRC Press, 2012, 568 p.

[16] N. A. Korotkova, "Optimizaciya parametrov kremnievih mikrostripovih detektorov: avtoreferat, " Moscow: MGU, 2006, 141 p. [in Russian]

[17] K. Hartman, E. Lezki, W. Schafer, "Statistische Versuchsplanung und -auswertung in der Stoffwirtschaft,"Leipzig : VEB Deutscher Verlag fur Grundstoffindustrie, 1974, 439 p.